



UNIVERSITY OF LEEDS

This is a repository copy of *Performance-based iterative learning control for task-oriented rehabilitation: a pilot study in robot-assisted bilateral training*.

White Rose Research Online URL for this paper:

<https://eprints.whiterose.ac.uk/176028/>

Version: Accepted Version

Article:

Miao, Q, Li, Z, Chu, K et al. (4 more authors) (2021) Performance-based iterative learning control for task-oriented rehabilitation: a pilot study in robot-assisted bilateral training. IEEE Transactions on Cognitive and Developmental Systems. p. 1. ISSN 2379-8920

<https://doi.org/10.1109/tcds.2021.3072096>

© 2021 IEEE. Personal use of this material is permitted. Permission from IEEE must be obtained for all other uses, in any current or future media, including reprinting/republishing this material for advertising or promotional purposes, creating new collective works, for resale or redistribution to servers or lists, or reuse of any copyrighted component of this work in other works.

Reuse

Items deposited in White Rose Research Online are protected by copyright, with all rights reserved unless indicated otherwise. They may be downloaded and/or printed for private study, or other acts as permitted by national copyright laws. The publisher or other rights holders may allow further reproduction and re-use of the full text version. This is indicated by the licence information on the White Rose Research Online record for the item.

Takedown

If you consider content in White Rose Research Online to be in breach of UK law, please notify us by emailing eprints@whiterose.ac.uk including the URL of the record and the reason for the withdrawal request.



eprints@whiterose.ac.uk
<https://eprints.whiterose.ac.uk/>

Performance-based iterative learning control for task-oriented rehabilitation: a pilot study in robot-assisted bilateral training

Qing Miao, *Member, IEEE*, Zhijun Li, *Senior Member, IEEE*, Kaiya Chu, Yudong Liu, Yuxin Peng, Sheng Q. Xie, *Senior Member, IEEE*, Mingming Zhang*, *Senior Member, IEEE*

Abstract—Active participation from human subjects can enhance the effectiveness of robot-assisted rehabilitation. Developing interactive control strategies for customized assistance is therefore essential for encouraging human-robot engagement. However, existing human-robot interactive control strategies lack precise evaluation indicators with effective convergence method to steadily and rapidly customize appropriate assistance during task-oriented training. This study proposes a performance-based iterative learning control algorithm for robot-assisted training, which aims at providing subject-specific robotic assistance to encourage active participation. Three performance indicators based on a Fugl-Meyer Assessment (FMA) regression model are introduced to associate clinical scales with robot-based measures, and a fuzzy logic is employed for comprehensive performance evaluation. To increase efficient training time, a piecewise learning rate based iterative law is applied to quickly converge to a subject-specific control parameter session by session. The proposed strategy is preliminarily estimated for a case of bilateral upper limb training with an end-effector based robotic system. Experimental results with human subjects indicate that the proposed strategy can obtain appropriate parameters after only several iterations and adapt to random perturbations (like muscle fatigue).

Index Terms—Bilateral upper limb, performance-based, robot-assisted rehabilitation, subject-specific, training task planning.

NOMENCLATURE

| | |
|-----------------|---|
| L_b | Distance between the handles. |
| P_c | Center position of L_b . |
| q_d | Desired position. |
| q_m | Measured position. |
| F | Interactive force. |
| M, B, K | Admittance parameters. |
| P_n, S_n, D_n | Measured peakspeed, smoothness, and duration of the n^{th} round. |

| | |
|-----------------------------------|--|
| P_d, S_d, D_d | Desired peakspeed, smoothness, and duration. |
| $P_{thr}, S_{thr}, D_{thr}$ | Peakspeed, smoothness, and duration thresholds. |
| a, b | Fitts's law parameters. |
| L | Distance between the targets. |
| R | Radius of the targets. |
| U_P, U_S, U_D | Universe of discourse of performance errors. |
| $\lambda_P, \lambda_S, \lambda_D$ | Proportionality coefficients. |
| μ_E | Output linguistic variable. |
| z | Non-fuzzy output value. |
| ρ_n | Iterative learning rate of the n^{th} round. |
| E_n | Comprehensive performance error of the n^{th} round. |

I. INTRODUCTION

Developing an effective rehabilitation strategy is one of the most significant aspects of research on motor recovery [1]-[4]. Conventional rehabilitation interventions mainly rely on one-on-one therapy by physiotherapists. However, this manual training lacks efficient outcomes owing to its great work intensity and poor repeatability [5]. To address this issue, robot-assisted rehabilitation has been increasingly reported [6]-[9].

Unlike isolated robotic systems in which the devices only need to perform high tracking precision and control stability [10]-[12], another key principle should be taken into account in rehabilitation robots, that is developing assistive strategies to improve patients' active participation during the training. Current evidence indicates that training with a high level of engagement contributes to the remodeling of the premotor cortex [13]. Therefore, providing tailored robotic assistance to

We acknowledge the funding supports from the National Natural Science Foundation of China (Grant No. 61903181), the Research Foundation of Guangdong Province (Grant No. 2020ZDZX3001), Shenzhen-Hong Kong Institute of Brain Science-Shenzhen Fundamental Research Institutions (Grant No. 2021SHIBS0002), and Shenzhen Key Laboratory of Smart Healthcare Engineering (Grant No. ZDSYS20200811144003009). We would like to thank Southern University of Science and Technology for providing financial support for conducting this study. (*Corresponding author: Mingming Zhang).

Q. Miao, K. Chu, L. Liu and M. Zhang are with Shenzhen Key Laboratory of Smart Healthcare Engineering, Southern University of Science and Technology, Shenzhen 518055, China, and also with Department of Biomedical

Engineering, Southern University of Science and Technology, Shenzhen, 518055, China (e-mail: miaoq@sustech.edu.cn; chuky@mail.sustech.edu.cn; l1710118@mail.sustech.edu.cn; zhangmm@sustech.edu.cn).

Z. Li is with the School of Information Science and Technology, University of Science and Technology of China, Hefei 230026, China. (e-mail: zjli@ieee.org).

Y. Peng is with the Department of Physical Education and Sports Science, Zhejiang University, Hangzhou 310028, China. (e-mail: yxpeng@zju.edu.cn).

Sheng Q. Xie is with the School of Electronic and Electrical Engineering, University of Leeds, Leeds, United Kingdom. (e-mail: S.Q.Xie@leeds.ac.uk).

involvement and recovery by designing appropriate human-robot interaction controllers is particularly significant.

Impedance/admittance control was developed as a baseline control method to perform compliant human-robot cooperation [14]-[18]. On that basis, several advanced strategies were further exploited with adaptive laws to provide appropriate assistance only when patients cannot accomplish training tasks, which is also known as “assist-as-needed (AAN)” control techniques [19]-[24]. Pehlivan, et al. [23] proposed a minimal AAN controller for wrist rehabilitation robots, in which the adaptive input estimation scheme included extended Kalman filter with Lyapunov stability analysis. The experimental results on healthy subjects showed that the algorithms could promote active participation of subjects with varying degrees of impairment. Luo, et al. [24] proposed a Gaussian radial basis function (RBF) networks-based method to quantify the degree of users’ impairment, and a greedy principle was employed to update the networks to increase human active engagement. Agarwal and Deshpande [25] developed two adaptive impedance controllers to provide accurate torque assistance to a subject. A neural-network-based force-field model was built to assist the finger motion to follow a target trajectory, and a radial basis function (RBF) network was used to provide a feedforward assistance for accurate trajectory tracking. Zhang, et al. [26] proposed a reinforcement learning-based impedance controller to achieve AAN training, where the stiffness of the force-field was regulated based on the trajectory tracking errors. The proposed controller implemented an actor-critic structure to avoid the requirement of the prior knowledge. While the above-mentioned studies achieved good results, using a single variable, such as trajectory tracking error, movement velocity, or interactive force, has limited reliability and stability to accurately estimate subjects’ motor functions. In this case, the robotic system has more possibility of providing unsuitable assistance, which may cause patients’ negative emotion or intermittent slack during the training. Thus, it is important to evaluate motion state accurately to formulate robotic subject-specific assistance for maximizing active participation of the patients.

To address this issue, performance-based control strategies have been proposed [27], [28]. These strategies are dependent on multiple kinematics indicators to comprehensively evaluate subjects’ motor functions, and adaptive controllers are designed to optimize robotic assistance based on the evaluation results. Krebs, et al. [27] detailed a concept of performance-based progressive robot therapy with MIT-MANUS, which included four diverse indicators in task-oriented training. A piecewise function was adopted as an adaptive algorithm to tune the task difficulty. Similarly, Papaleo, et al. [28] presented a patient-tailored approach by using a 7 degrees of freedom (DOFs) robot arm for three dimensional (3D) upper limb training. Three different performance indicators were developed to evaluate motor ability through a weighted sum method. Although these objective measures appear to be useful, they are not tightly linked to widely accepted clinical scales, such as Fugl-Meyer Assessment (FMA), the Motor Status Score (MSS), or the modified Ashworth Scale, which may reduce the evaluation

reliability of limbs’ motor ability. Additionally, using fixed weights based linear combination or simple piecewise function cannot guarantee that the control parameters will converge to some stable values, which potentially leads to frequent changes of robotic assistance. This negative robotic intervention would affect patients’ active engagement and even bring about unsafe training process.

In this study, we propose a performance-based iterative learning control strategy to adaptively and rapidly convergent to subject-specific training difficulty levels. Three kinematic parameters of a FMA regression model are applied as the measurement indicators to characterize subjects’ motor functions, and a fuzzy logic is involved as an information fusion technique for comprehensive evaluation of the performance. Finally, a piecewise learning rate based iterative law is employed to optimize control parameters to achieve subject-specific. Compared with prior studies, the main contributions of the paper include the following.

1) Clinical scales related measures can improve the reliability of the performance evaluation for limb’s motor ability and avoid the multicollinearity between the evaluation indicators. Besides, using fuzzy logic can help to establish a precise and quantitative evaluation model.

2) A piecewise learning rate based iterative method can speed up searching process for optimal parameters and remain the convergence procedure stable, which contributes to increasing efficient training time.

II. METHODS

A. System Configuration

The robotic device is a platform for human bilateral upper limb training with three degrees of freedom (DOFs). It comprises two components, including a motion module and two hand holders. The motion module consists of three mutually perpendicular linear slide systems that with the aim to transfer the rotatory motion of the motors to the linear motion of the eight sliders by using six dustless linear motion modules. The hand holders are respectively and rigidly connected with sliders through two three-axis force sensors.

The predefined data on the PC are transferred to the main control platform CompactRIO through an ethernet network. The output signals of CompactRIO are used to control the servo system. Then, the servo system provides position feedback in the form of pulse signals to the CompactRIO based on a digital acquisition module. Two three-axis force sensors are installed to measure real-time human-robot interaction, thereby facilitating the interactive bilateral upper limb training. For training safety, a series of photoelectric switches are set up at the side edges of the dustless linear motion modules. They are also used as a reference to set the starting position of the hand holders.

B. Task and Performance Indicators

The proposed robot-assisted bilateral training strategy is presented in Fig. 1. During the training, the subject is asked to straightly stand on the ground, grasp the handles, and focus on

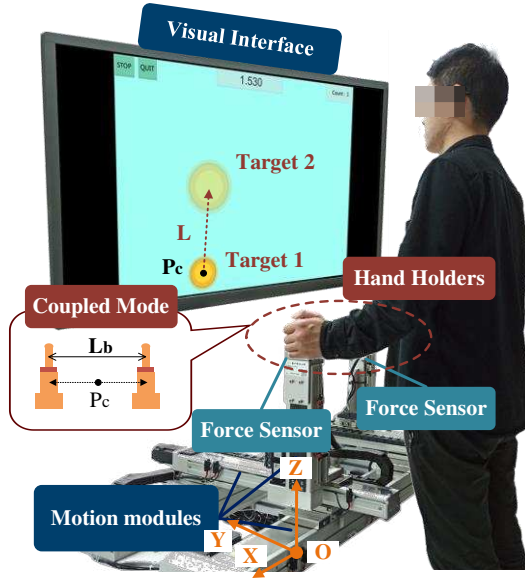


Fig. 1. Schematic diagram of the proposed training strategy. The orange arrowed lines refer to the global coordinate system. The distance between two handles is fixed as L_b . The parameter P_c is the center position between the handles. As shown in the visual interface, the parameter L represents the distance between any two targets.

the training task shown on the visual interface. The handles are coupled as a link by programming, where the distance is denoted as L_b . The synchronous movement of the handles is actuated by the resultant force. The task is a two-dimensional target-to-target reaching training, as shown in Fig. 1. The annulus with light orange shadows denotes the targets. Each target's position P_c is located at the center of the robotic handles. After reaching one target, another random target will be generated for a new round in the same session of the training. To make each round of the training consistent, the distance between any two targets is equal, denoted as L .

To quantize the performance of target-to-target task, Bosecker, et al. [29] built a detailed FMA model by using linear regression analysis based on clinical data from 111 chronic stroke subjects, which is obtained in (1),

$$FMA = -22.39 + 44.04 \cdot P_n + 112.94 \cdot S_n + 2.15 \cdot D_n - 20.00 \cdot J_n \quad (1)$$

where the parameter P_n represents peakspeed, defined as the maximum speed of movement. The parameter S_n is smoothness, defined as the ratio mean value of speed to the peak value. The parameter D_n denotes duration, which is the completion time of the n^{th} round of the training task. The parameter J_n means joint independence, and it is mainly applied for circle drawing task evaluation. Considering that the proposed training strategy belongs to the reaching task, the former three indicators are adopted to evaluate the training performance of the subjects' motor functions.

C. Control System with Adaptation

The control system consists of an admittance law module, a position controller, a performance acquisition module, a fuzzy logic module, and an iterative tuning module, as presented in

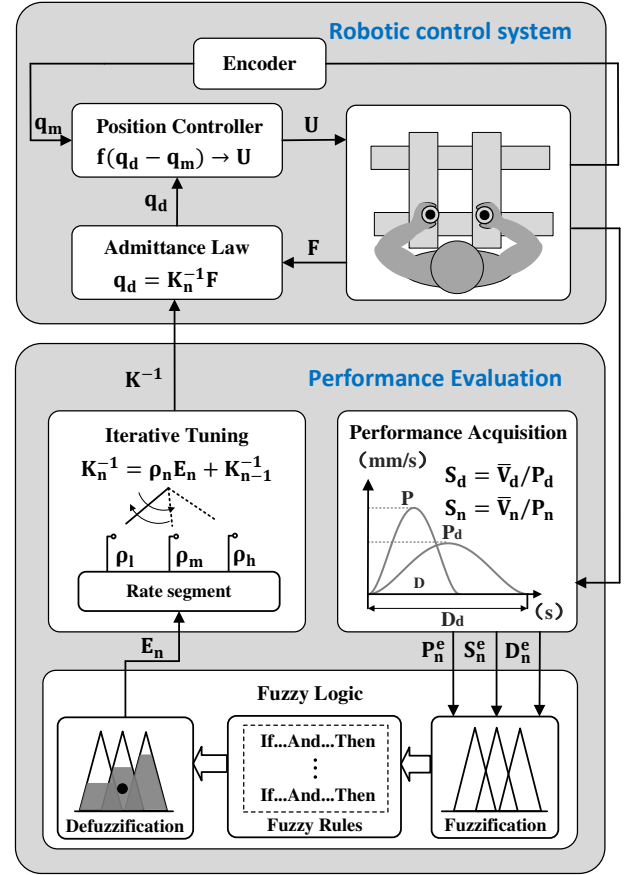


Fig. 2. Control diagram of the robotic system. The measured parameter F is the vector of human-machine interactive forces on the X-axis and the Y-axis. The output of the admittance law q_d is the vector of the desired position, and q_m is the vector of the measured position. The output of the PID controllers U is the vector of voltage, which is the input for motors. For the performance evaluation, the parameters P_n^e , S_n^e and D_n^e are performance evaluation indicators corresponding to the errors of peakspeed, smoothness, and duration in the n^{th} training round. Then, the fuzzy logic is to obtain a comprehensive performance error E_n . After tuning the K_n^{-1} by iterative learning, the modified admittance parameter K_{n+1}^{-1} can be calculated and used in the $(n+1)^{\text{th}}$ training round.

Fig. 2.

The admittance law module makes the device operate with specific inertia, specific damping, and unfixed stiffness by measuring and controlling the force from two force sensors. These parameters are equal on the X-axis and the Y-axis. The admittance equation is written as in (2).

$$q_d = \frac{F}{Ms^2 + Ds + K} \quad (2)$$

$$F = F_l + F_r \quad (3)$$

Here, $F = [F_x \ F_y]^T$ denotes the measured interactive force vector along the X-axis and the Y-axis, which is determined by the forces applied on the left handle $F_l = [F_l^x \ F_l^y]^T$ and the right handle $F_r = [F_r^x \ F_r^y]^T$, as shown in (3). Setting $q_d = [q_d^x \ q_d^y]^T$ as the desired position vector caused by the interactive forces, the admittance law can be simplified into (4) as a linear spring, where $M = D = 0$ [30].

$$q_d = K^{-1}F \quad (4)$$

The position controller is used to convert the desired position vector into the required motor voltage $U = [U^x \ U^y]^T$.

In terms of the performance acquisition module, the measured performance P_n , S_n and D_n will be worked out when the n^{th} round of the task is accomplished, as in (5) to (7),

$$P_n = \max \left\{ \frac{d\|{}^1_n q_d\|_2}{dt}, \frac{d\|{}^2_n q_d\|_2}{dt}, \dots, \frac{d\|{}^m_n q_d\|_2}{dt} \right\} \quad (5)$$

$$S_n = \frac{\bar{v}_n}{P_n} = \frac{\frac{\sum_{i=1}^m \|{}^i_n q_d\|_2}{\sum_{i=1}^m \|{}^i_n t\|_2}}{\max \left\{ \frac{d\|{}^1_n q_d\|_2}{dt}, \frac{d\|{}^2_n q_d\|_2}{dt}, \dots, \frac{d\|{}^m_n q_d\|_2}{dt} \right\}} \quad (6)$$

$$D_n = \frac{1}{m} \sum_{i=1}^m i t \quad (7)$$

where the parameter ${}^i_n q_d$ is the i^{th} desired position vector in the n^{th} round on X-axis and Y-axis, respectively. The parameter ${}^i_n t$ represents the corresponding time. The parameter m is the sample number in one round. Then, the performance errors can be calculated based on three measured performance indicators with desired task performance as in (8) to (10),

$$P_n^e = \begin{cases} P_d - P_n, P_n^e \in [-P_{thr}, P_{thr}] \\ P_{thr}, P_n^e \in (P_{thr}, +\infty) \\ -P_{thr}, P_n^e \in (-\infty, P_{thr}) \end{cases} \quad (8)$$

$$S_n^e = \begin{cases} S_d - S_n, S_n^e \in [-S_{thr}, S_{thr}] \\ S_{thr}, S_n^e \in (S_{thr}, +\infty) \\ -S_{thr}, S_n^e \in (-\infty, S_{thr}) \end{cases} \quad (9)$$

$$D_n^e = \begin{cases} D_n - D_d, D_n^e \in [-D_{thr}, D_{thr}] \\ D_{thr}, D_n^e \in (D_{thr}, +\infty) \\ -D_{thr}, D_n^e \in (-\infty, D_{thr}) \end{cases} \quad (10)$$

where parameters P_d , S_d , D_d are the desired peakspeed, smoothness and duration. P_{thr} , S_{thr} and D_{thr} are corresponding threshold values to limit the maximum and minimum ranges of variations. To make the thresholds appropriate, a physiotherapist is involved to give basic references at first. Then, they are further adjusted according to the feedbacks of the subjects after a series of previous experiments.

For the calculation procedure of the desired performance indicators, the Fitts's law is used to define D_d of one round as in (11) [31],

$$D_d = a + b \cdot \log_2 \left(\frac{L}{R} \right) \quad (11)$$

where R denotes the radius of the targets, and L represents the distance between any two targets. The parameters a and b are

constant values, which are commonly set according to clinical training requirements.

Considering that the training belongs to the type of reaching task, the minimum jerk principle is involved to associate the motion time with the displacement as in (12) [32],

$$Q = L \cdot \left(\frac{10t^3}{T^3} - \frac{15t^4}{T^4} + \frac{6t^5}{T^5} \right) \quad (12)$$

where the parameter T is equivalent to D_d . To further analyze the speed variables, the equation (13) can be obtained by taking the derivative of (12).

$$V = Q' = L \cdot \left(\frac{30t^2}{D_d^3} - \frac{60t^3}{D_d^4} + \frac{30t^4}{D_d^5} \right) \quad (13)$$

Then, the parameter P_d can be calculated as in (14)

$$P_d = \max(V) \quad (14)$$

Further, the desired mean speed can be written as in (15)

$$\bar{v}_d = \frac{L}{D_d} \quad (15)$$

Finally, the parameter S_d is adapted as followed

$$S_d = \frac{\bar{v}_d}{P_d} \quad (16)$$

The fuzzy logic module has a function of multi-information fusion for a multiple-input single-output system to obtain a comprehensive performance error. In general, the fuzzy logic mainly consists of three stages, including fuzzification, fuzzy inference, and defuzzification. The stage of fuzzification is the process of conversing the inputs and the output into membership functions. The inputs of the fuzzy logic module are above-mentioned performance errors P_n^e , S_n^e , D_n^e , and the output is the comprehensive performance error, denoted as E_n . To define the linguistic variables, the range of variations of the inputs need to be transformed into normalized universe of discourses, which can be calculated based on linear transformation as in (17),

$$\begin{cases} U_P = [-\lambda_P P_{thr}, \lambda_P P_{thr}] \\ U_S = [-\lambda_S S_{thr}, \lambda_S S_{thr}] \\ U_D = [-\lambda_D D_{thr}, \lambda_D D_{thr}] \end{cases} \quad (17)$$

where λ_P , λ_S , λ_D are proportionality coefficients. In this study, the universe of discourse is set as $[-6, 6]$ for both inputs and the output. The fuzzification of the inputs and outputs was through the triangular membership functions shown in Fig.3. Each input consists of three linguistic variables, denoted as E (easy), M (medium), and H (hard). The output variable has five linguistic variables, corresponding to BE (big easiness), SE (small easiness), NC (no change), SD (small difficulty), and BD (big difficulty). The parameters of each membership function were defined by the combination of the reference [33] and the pre-experiments, whose shape is an isosceles triangle and the overlap between two adjacent membership functions is 50%.

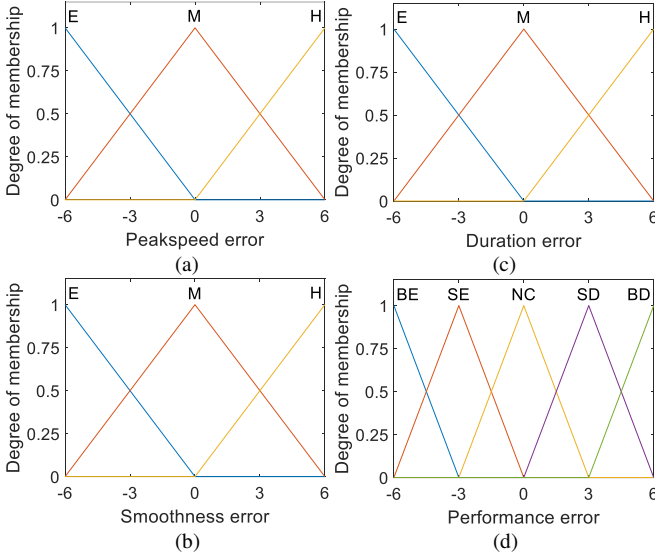


Fig. 3. The membership functions of the input and the output variables. (a) The fuzzy peakspeed error. (b) The fuzzy smoothness error. (c) The fuzzy duration error. (d) The output membership function.

The stage of fuzzy inference is to obtain linguistic variables of the output based on the fuzzified inputs and the fuzzy rules. The fuzzy rules commonly depend on experience to establish the mapping relationship between fuzzified inputs and the output, commonly using fuzzy language as “IF...AND...AND...THEN”. Table I lists the fuzzy output obtained by 27 combinations of the three fuzzy sets of input variables. The fuzzy rules are first developed by the weight relationship among the performance measures in (1) and further tuned through experiments. The Mamdani’s max-min method [34] is used for the inference process. Then, the membership degree resulted by each of the possible combinations is calculated first as in (18),

$$\mu_E^j = \min\{\mu_P^j, \mu_S^j, \mu_D^j\}, j = 1, 2, \dots, l \quad (18)$$

where j is the number of possible combinations of input linguistic variables that lead the j^{th} output linguistic variable. $\mu_P^j, \mu_S^j, \mu_D^j$ are the corresponding input linguistic variables to μ_E^j . The membership degrees of the output linguistic variable can be calculated as in (19).

$$\mu_{E_i} = \max\{\mu_E^1, \mu_E^2, \dots, \mu_E^l\} \quad (19)$$

Finally, the stage of defuzzification is to convert the membership degrees of the output linguistic variable to the exact values for comprehensive performance evaluation. The centroid of area method is applied in this process to obtain more smooth output, as in (20),

$$z = df(z) = \frac{\int_{a_e}^{b_e} z \mu_E(z) dz}{\int_{a_e}^{b_e} \mu_E(z) dz} \quad (20)$$

where z is the non-fuzzy output value. a_e and b_e are the lower and upper bounds of the area.

The iterative tuning module is used to modify the admittance parameter to guarantee the convergence of the n^{th}

TABLE I
THE RULE TABLES FOR THE FUZZY LOGIC.

| No. | P_n^e | S_n^e | D_n^e | E_n | No. | P_n^e | S_n^e | D_n^e | E_n |
|-----|---------|---------|---------|-------|-----|---------|---------|---------|-------|
| 1 | E | E | E | BE | 15 | M | M | H | NC |
| 2 | E | E | M | BE | 16 | H | M | E | NC |
| 3 | E | E | H | BE | 17 | H | M | M | NC |
| 4 | M | E | E | BE | 18 | H | M | H | SD |
| 5 | M | E | M | SE | 19 | E | H | E | SD |
| 6 | M | E | H | SE | 20 | E | H | M | SD |
| 7 | H | E | E | SE | 21 | E | H | H | SD |
| 8 | H | E | M | SE | 22 | M | H | E | SD |
| 9 | H | E | H | SE | 23 | M | H | M | SD |
| 10 | E | M | E | SE | 24 | M | H | H | BD |
| 11 | E | M | M | SE | 25 | H | H | E | BD |
| 12 | E | M | H | SE | 26 | H | H | M | BD |
| 13 | M | M | E | SE | 27 | H | H | H | BD |
| 14 | M | M | M | NC | | | | | |

Note: Total 27 fuzzy rules are listed in Table I. The input and the output linguistic variables are shaded in light blue and light red, respectively.

comprehensive performance error E_n to zero with actions session by session, which can be described as in (21),

$$K_{n+1}^{-1} = K_n^{-1} + \rho_n E_n \quad (21)$$

where ρ_n is the iterative learning rate. It should be noted that a small ρ_n will increase the training rounds to converge, which affects the training effectiveness. In contrast, a big ρ_n will generate oscillations of the parameter, which may reduce the training safety and comfort. Accordingly, a piecewise function is developed to switch the various iterative learning rates based on E_n as in (22),

$$\rho_n = \begin{cases} \rho_l, & |E_n| \in [0, E_n^l) \\ \rho_m, & |E_n| \in [E_n^l, E_n^h) \\ \rho_h, & |E_n| \in [E_n^h, E_{thr}] \end{cases} \quad (22)$$

where E_n^l and E_n^h are segment points to classify E_n into three levels, and ρ_l, ρ_m, ρ_h are corresponding iterative learning rates. The parameter E_{thr} is the output threshold.

III. EXPERIMENTAL RESULTS

A. Experimental Protocol

Eight healthy subjects (eight males: age 27.33 ± 4.73 , height 1.76 ± 0.04 m, weight 76.00 ± 12.29 kg) volunteered to participate in this study. The study was approved by the Southern University of Science and Technology, Human Participants Ethics Committee (20190004) and consents were obtained from all participants. During the experiments, each participant was required to actively reach 50 targets displayed on the screen.

In terms of the robotic device, the distance between two handles was set as $L_b = 350$ mm. Due to all the subjects being healthy individuals, the initial K_0^{-1} was set at 0.1, and the range of K_n^{-1} was limited in $[0, 0.12]$. To guarantee the safety of the training, a stop button was provided for subjects to instantly shut down the system. In order to test the performance of the proposed control strategy, the experiments were divided into three blocks.

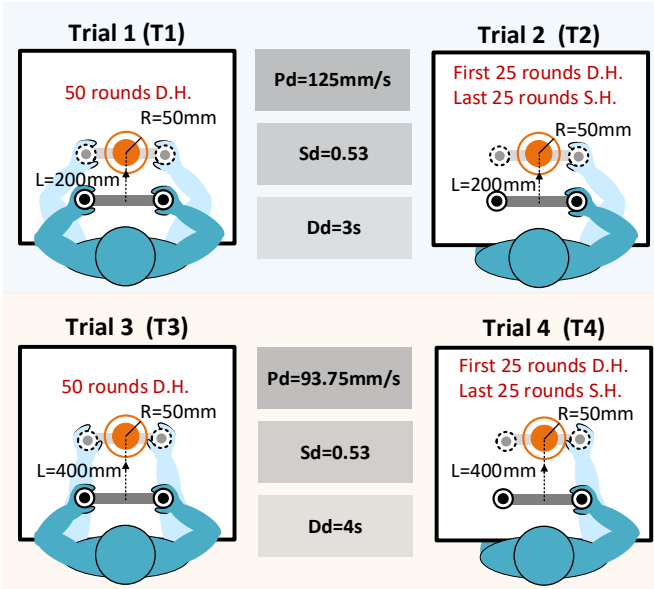


Fig. 4. Four different experimental trials. The orange circle represents the target, where its radius is denoted as R . In T1, subjects should accomplish 50 rounds training using double hands (D.H.) in nature way with indicators $P_d=125\text{mm/s}$, $S_d=0.53$ and $D_d=3\text{s}$. Based on the same level of performance requirement, T3 asked the subjects to complete the task employing double hands in first 25 rounds, and single hand (S.H.) in last 25 rounds. T3 and T4 were designed with the same training modes as T1 and T2, respectively. To further validate the proposed strategy, a different level of performance indicators was defined as $P_d=93.75\text{mm/s}$, $S_d=0.53$ and $D_d=4\text{s}$.

The first experiment was conducted to estimate the feasibility of using three mentioned performance measures in robot-assisted training, including four trials on eight subjects, as shown in Fig. 4. In the first trial (T1), the distance between any two targets was set as $L=200\text{mm}$, and the radius of the targets was set as $R=50\text{mm}$. According to a series of preliminary training tests, the parameters a and b in Fitts's law were set both at 1. Combined with equations (11) to (16), the desired performance indicators can be worked out as $P_d=125\text{mm/s}$, $S_d=0.53$ and $D_d=3\text{s}$, respectively. During T1, all the subjects were asked to execute the training task with double hands in their natural ways. In the second trial (T2), the training parameters and the desired performance indicators were set as equal as the values in T1. All the subjects should perform with the same requirement during the first 25 rounds, while they were required to complete the last 25 rounds with only one hand to simulate the situation of muscle fatigue. For the third trial (T3) and the fourth trial (T4), the training modes were designed as similar to T1 and T2, while the parameter L was changed to 400mm. Accordingly, the desired performance indicators were redefined as $P_d=93.75\text{mm/s}$, $S_d=0.53$, and $D_d=4\text{s}$, correspondingly. In these four trials, P_{thr} , S_{thr} , D_{thr} were set at 30mm/s, 0.15, 1.5s, respectively. For the iterative tuning module, the range of E_n was set between -0.03 and 0.03, and the segment points E_n^l and E_n^h were separately set as 0.02 and 0.03. The iterative learning rates were set as $\rho_l=0.4$, $\rho_m=0.5$, $\rho_h=0.6$.

The second experiment was designed to verify whether the fuzzy logic is more effective than the weighted sum in comprehensive evaluation of motor ability. The subject was

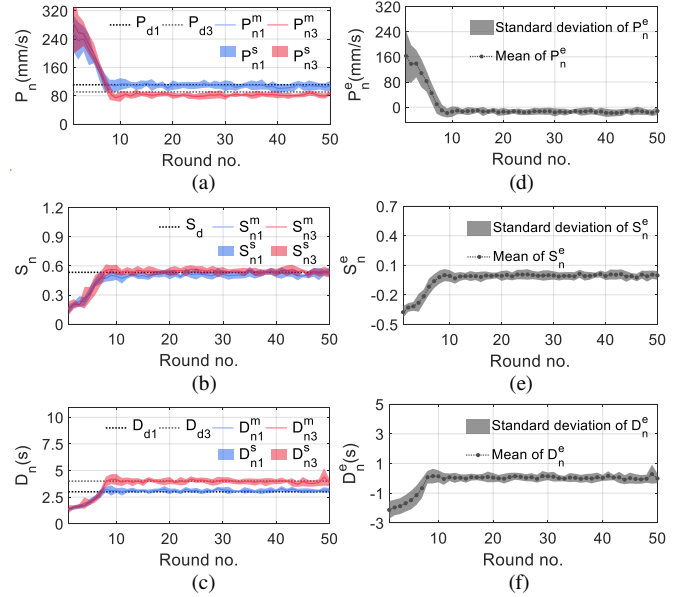


Fig. 5. The results of measured performance indicators applied by eight subjects in T1 and T3. The black and grey imaginary lines represent different desired performance indicators. Fig. 5 (a) to Fig. 5 (c) use red and blue lines to represent the mean values of measured performance indicators, and apply light blue and light red shadows to describe the standard deviations. Fig. 5 (d) to Fig. 5 (f) represent the results of corresponding errors, where the grey lines with dots represent mean values, and the grey shadows represent standard deviations.

required to conduct the training task as same as in T1 with a weighted sum method rather than fuzzy logic. The weighted sum was expressed as in (23)

$$E_n = \omega_p \tilde{P}_n^e + \omega_s \tilde{S}_n^e + \omega_d \tilde{D}_n^e \quad (23)$$

where \tilde{P}_n^e , \tilde{S}_n^e , \tilde{D}_n^e represent the normalized performance errors, limited in the range of $[-1, 1]$. The corresponding weights $\omega_p=0.28$, $\omega_s=0.71$, $\omega_d=0.01$ were designed according to the proportional relation among P_n , S_n , D_n in (1) by linear scaling.

In the third experiment, one subject was required to execute two trials with same training requirement with T1, but with two different levels of fixed learning rates ($\rho=0.4$ and $\rho=0.6$). The purpose of this experiment is to validate the advantages of implementing the piecewise rates compared with the fixed rates in convergence of K^{-1} .

B. Experimental Results

Fig. 5 reports the results of desired and measured performance indicators in T1 and T3. It can be seen that all the measured performance indicators are close to the desired values after 10 training rounds. For quantitative analysis, Fig. 5 (d) to Fig. 5 (f) show the corresponding average tracking errors. The values of the root-mean-square error (RMSE) from the 10th round to the 50th round in two trials are 14.27mm/s, 0.01, and 0.08s, which are all in the range of the desired performance thresholds. The measured interactive forces in T1 and T3 are given in Fig. 6. The results show that the forces vary with small fluctuations during the last 40 rounds in both two trials, which intuitively reflects stable interaction between the subjects and the robotic system during the training. Fig. 7 depicts the variations of K^{-1} , which can be found that all K^{-1} values

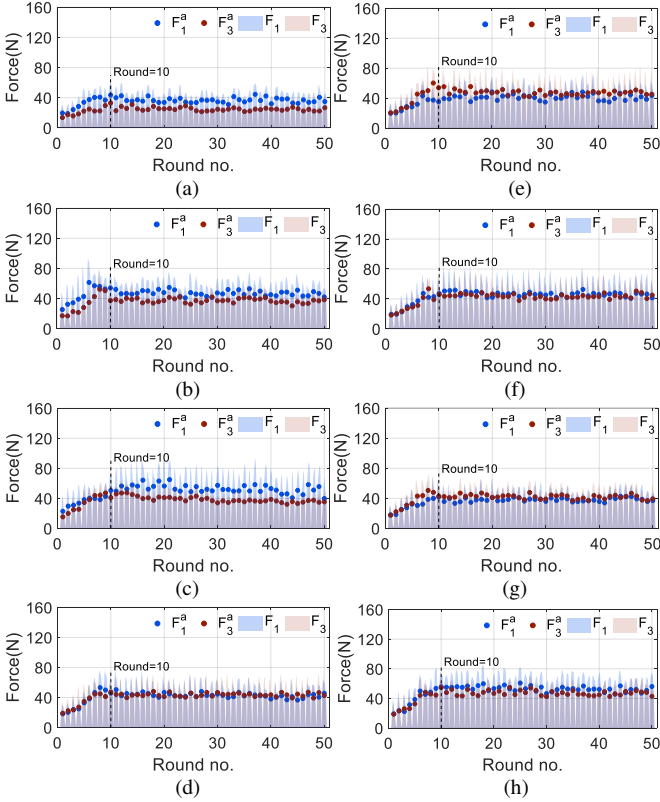


Fig. 6. The results of measured interactive forces in T1 and T3. Fig. 6 (a) to Fig. 6 (h) represent the results of eight subjects, where the light blue and light red shadows represent measured forces F_1 and F_3 in T1 and T3, respectively. To make it clear, the blue and red dots are used to show the corresponding average forces in 50 training rounds, which are denoted as F_1^a and F_3^a .

rapidly reduce from 0.1 at the first 7 rounds and moderately adjust in the next 2 rounds. Then, they converge to various levels and slightly float around them. Statistical results of the convergent parameters are summarized in Table II. On one hand, the data imply that the system has a function of adaptively adjusting the parameter to help the same subject handle training tasks with diverse difficulties. On the other hand, the results indicate that the system can specify customized control parameters for individuals according to their different athletic abilities.

Fig. 8 reports the results of desired and measured performance indicators in T2 and T4. The variation trends of the measured indicators are similar to the results from the 10th round to the 25th round in T1 and T3, while a large fluctuation appears in the next 5 rounds and then return to be stable. This phenomenon can be explained by the switching from double hands to the single hand. The results of the RMSE values from the 10th round to the 25th round in two trials are 16.21 mm/s, 0.01, 0.15s, and 15.63mm/s, 0.02, 0.16s during the last 20 rounds. Fig. 9 presents the eight subjects' results of applied interactive forces. It can be seen that the average forces of all the subjects in the last 25 rounds are distinctly smaller than the values in the first 25 rounds. The results of the convergent parameters are summarized in Table III and Table IV. A statistical analysis with paired-T test is used for comparisons among the trials. The result given in Fig. 10 shows that no significant difference is represented among these four trials from the 10th round to the

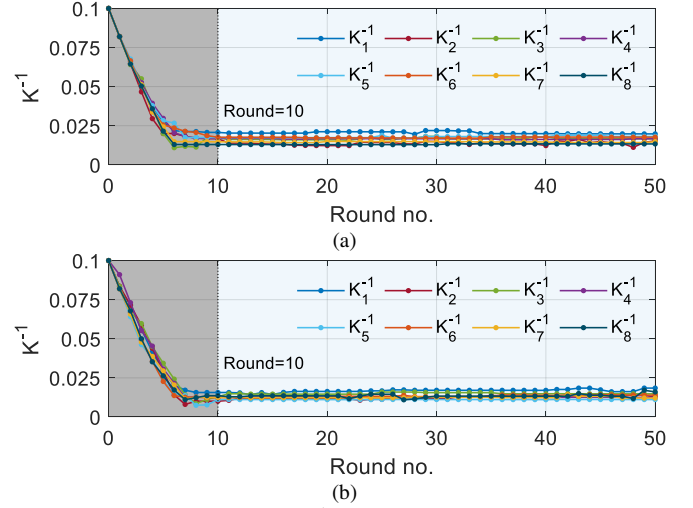


Fig. 7. The results of parameter K^{-1} in T1 and T3, being separately given in Fig. 7 (a) and Fig. 7 (b). The light grey shadow represents the searching region, and the light blue shadow represent the convergent region. The eight lines with dots are measured K^{-1} corresponding to eight subjects.

TABLE II
THE RESULTS OF STATISTICAL ANALYSIS FOR CONVERGENT PARAMETERS FROM THE 10TH ROUND TO THE 50TH ROUND IN T1 AND T3

| K | T1 | | T3 | |
|---|-------------------|--------|-------------------|--------|
| | Convergence Value | RMSE | Convergence Value | RMSE |
| 1 | 0.0205 | 0.0045 | 0.0167 | 0.0060 |
| 2 | 0.0166 | 0.0037 | 0.0149 | 0.0034 |
| 3 | 0.0138 | 0.0072 | 0.0123 | 0.0059 |
| 4 | 0.0165 | 0.0018 | 0.0126 | 0.0004 |
| 5 | 0.0179 | 0.0033 | 0.0111 | 0.0002 |
| 6 | 0.0146 | 0.0016 | 0.0125 | 0.0025 |
| 7 | 0.0175 | 0.0018 | 0.0133 | 0.0039 |
| 8 | 0.0132 | 0.0015 | 0.0134 | 0.0066 |

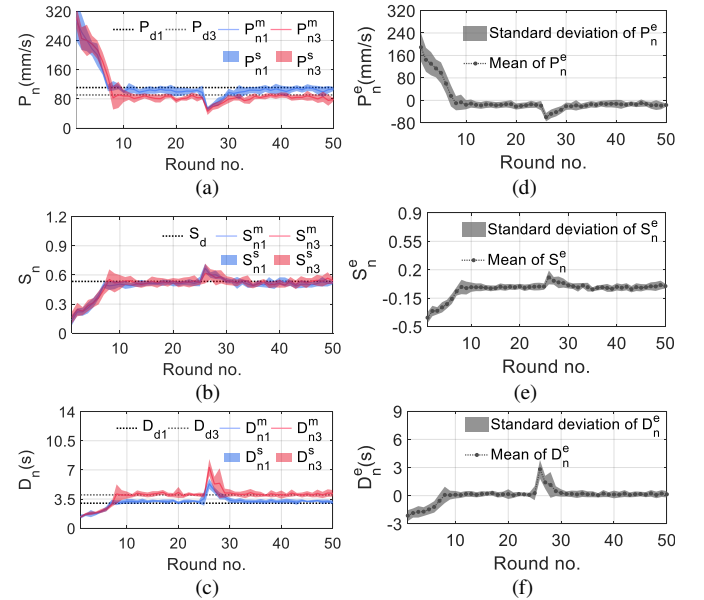


Fig. 8. The results of measured performance indicators applied by eight subjects in T2 and T4. The black and grey imaginary lines represent different desired performance indicators. Fig. 8 (a) to Fig. 8 (c) use red and blue lines to represent the mean values of measured performance indicators, and apply light blue and light red shadows to describe the standard deviations. Fig. 8 (d) to Fig. 8 (f) represent the results of corresponding errors, where the grey lines with dots represent mean values, and the grey shadows represent standard deviations.

25th round ($p=0.1625$), which would be possibly explained that

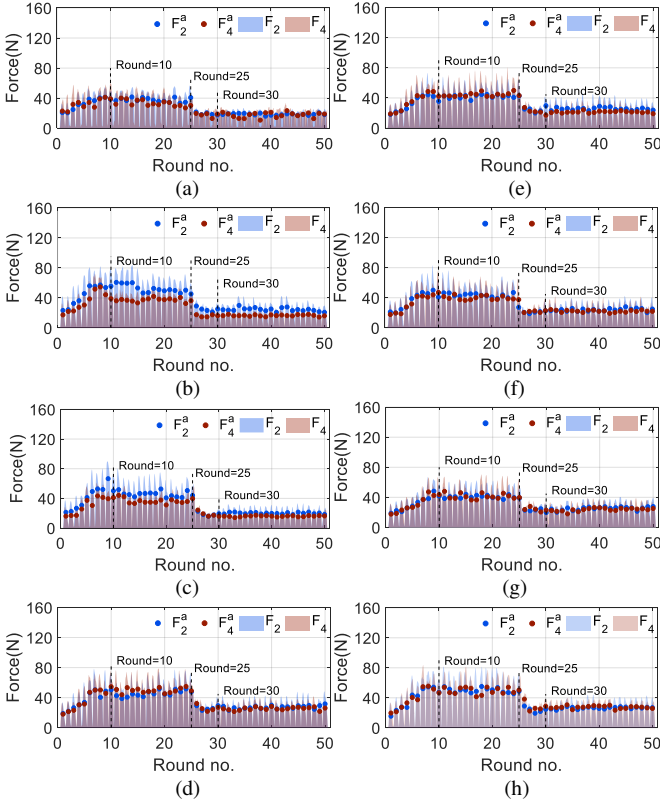


Fig. 9. The results of measured interactive forces in T2 and T4. Fig. 9 (a) to Fig. 9 (h) represent the results of eight subjects, where the light blue and light red shadows represent measured forces F_2 and F_4 in T2 and T4, respectively. To make it clear, the blue and red dots are used to show the corresponding average forces in 50 training rounds, which are denoted as F_2^a and F_4^a .

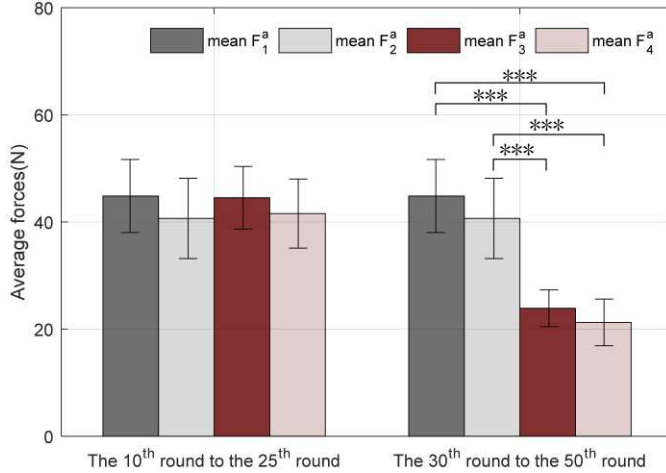


Fig. 10. The statistical analysis results of eight subjects' average during the convergent procedures in all trials. F_1^a , F_2^a , F_3^a , and F_4^a are the average forces performed from T1 to T4.

the output forces of the healthy individuals are similar. In contrast, the result shows significant differences between the training with double hands (T1 and T3) and the training with a single hand (T2 and T4) during the last 20 rounds, including the differences between T1 and T3 ($p=0.000031$), T1 and T4 ($p=0.000035$), T2 and T3 ($p=0.000036$), and T2 and T4 ($p=0.000025$). These significant differences imply that using a single to perform the movement successfully simulated the muscle fatigue. However, the more essential aspect is to analyze the stability of the interactive force, which can validate whether

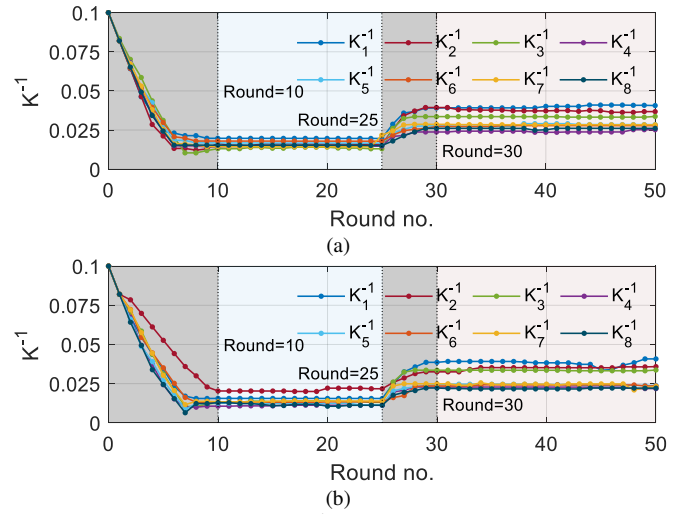


Fig. 11. The results of parameter K^{-1} in T1 and T3, being separately given in Fig. 11 (a) and Fig. 11 (b). The light grey shadows represent the searching regions, while the light blue and light red shadows represent two convergent regions in diverse phases. The eight lines with dots are measured K^{-1} corresponding to eight subjects.

the provided K^{-1} is appropriate for the subject. For this purpose, coefficient of variation was used to analyze the fluctuations of forces, denoted as the ratio of the standard deviation to the mean of the forces. It can be worked out that the mean values of c_v performed by eight subjects during the four trials' convergent procedures are $c_{v1}^m = 7.84\%$, $c_{v2}^m = 7.85\%$, $c_{v2}^{m*} = 7.39\%$, $c_{v3}^m = 7.48\%$, $c_{v4}^m = 8.15\%$, $c_{v4}^{m*} = 8.16\%$, which are all less than 0.1. Therefore, these small force fluctuations demonstrate that the subjects executed the training tasks well with appropriate control parameters. Fig. 11 presents parameter K^{-1} variations of eight subjects as similar as Fig. 7. The results show that each K^{-1} can converge to a certain value after around 10 training rounds from the beginning of both trials. After tuning for only about five rounds, the values newly converge to another levels, which have significant differences compared with the former K^{-1} values. It can be summarized that the system can adaptively provide optimized parameters for subjects who suffer from muscle fatigue. Psychologically, it is useful to improve engagement when people have negative feelings that they refuse to well perform in the whole training.

In the second experiment, the comparative results of K^{-1} via the weighted sum and the fuzzy logic are given in Fig. 12. It can be seen that the K^{-1} via the weighted sum rapidly reduce from 0.1 during the first 5 rounds, and moderately tune in next 5 rounds. However, it continuously varies during last 40 rounds, instead of converging to a certain value, which reflects that the robotic system kept tuning the training difficulty level all the time. For quantitative analysis, the K^{-1} via the fuzzy logic is 0.0146 ± 0.0003 , which shows better stability than the K^{-1} of the weighted sum method (0.0185 ± 0.0019). This suggests that using a precise evaluation model, like a weighted sum form, has limited robustness to uncertainties and anomalies during the training.

To further explore the effects of the learning rate on K^{-1} , the results of K^{-1} by using the fixed learning rates and the piecewise learning rate are presented in Fig. 13. It can be found

TABLE III
THE RESULTS OF STATISTICAL ANALYSIS FOR CONVERGENT PARAMETERS FROM THE 10TH ROUND TO THE 25TH ROUND IN T2 AND T4

| K | T2 | | T4 | |
|---|------------------|--------|------------------|--------|
| | Convergent Value | RMSE | Convergent Value | RMSE |
| 1 | 0.0197 | 0.0001 | 0.0155 | 0.0008 |
| 2 | 0.0135 | 0.0016 | 0.0135 | 0.0016 |
| 3 | 0.0159 | 0.0015 | 0.0209 | 0.0035 |
| 4 | 0.0147 | 0.0006 | 0.0110 | 0.0009 |
| 5 | 0.0167 | 0.0008 | 0.0123 | 0.0016 |
| 6 | 0.0148 | 0.0071 | 0.0137 | 0.0011 |
| 7 | 0.0179 | 0.0009 | 0.0133 | 0.0005 |
| 8 | 0.0153 | 0.0003 | 0.0116 | 0.0027 |

TABLE IV
THE RESULTS OF STATISTICAL ANALYSIS FOR CONVERGENT PARAMETERS FROM THE 30TH ROUND TO THE 50TH ROUND IN T2 AND T4

| K | T2 | | T4 | |
|---|------------------|--------|------------------|--------|
| | Convergent Value | RMSE | Convergent Value | RMSE |
| 1 | 0.0399 | 0.0035 | 0.0383 | 0.0079 |
| 2 | 0.0334 | 0.0007 | 0.0334 | 0.0007 |
| 3 | 0.0374 | 0.0037 | 0.0348 | 0.0046 |
| 4 | 0.0241 | 0.0024 | 0.0227 | 0.0017 |
| 5 | 0.0282 | 0.0030 | 0.0243 | 0.0016 |
| 6 | 0.0284 | 0.0004 | 0.0243 | 0.0046 |
| 7 | 0.0276 | 0.0011 | 0.0240 | 0.0014 |
| 8 | 0.0260 | 0.0015 | 0.0219 | 0.0011 |

that the K^{-1} via a small fixed learning rate converges and changes smoothly, while the declining process from the start value to the convergent value behaves slow, which could result in a reduction of the effective training time. In contrast, the K^{-1} by using a large fixed learning rate presents a big decreasing slope during the declining process. However, the variation of K^{-1} is sensitive. That is, a series of perturbations will be generated when some special circumstances, such as momentary desertion and occasional misoperation, which may cause discomfort for subjects. Employing the piecewise learning rate can make the declining process rapid and the convergent process smooth. Therefore, the results reflect that using a piecewise learning rate leads to a rapid and smooth convergence.

IV. DISCUSSION

The developed control strategy can benefit robot-assisted rehabilitation training in three aspects. Firstly, the control paradigm is capable of obtaining a subject-specific control parameter within a few training rounds, which avoids repeating modification and increases effective training time. Secondly, the proposed method can keep the convergent control parameter stable, while it can adaptively adjust the parameters to other values when the interactive situation changes, like natural muscle fatigue. Finally, rather than providing real-time assistance or correction, progressively modifying the control parameter can reduce the excessive intervention of the autogenic training, which is essential for motivation improvement and training safety.

Experiments on healthy subjects are enrolled to estimate the feasibility of the proposed control strategy. The results show that the performance-based iterative learning control is capable of providing different subject-specific parameters for

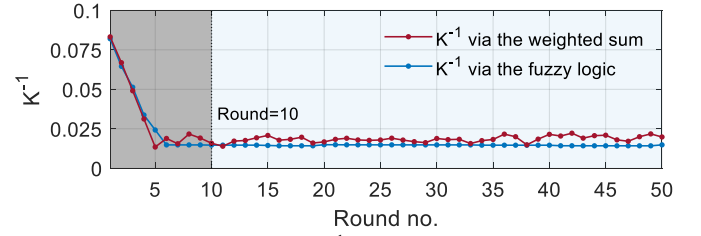


Fig. 12. The comparative result of K^{-1} via the weighted sum method and the fuzzy logic on one subject in T1. The light grey shadow represents the searching region, and the light blue shadow represent the convergent region.

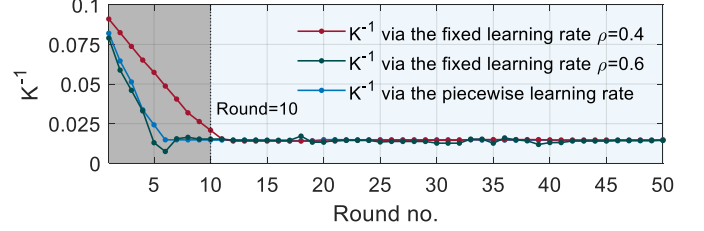


Fig. 13. The comparative results of K^{-1} via the fixed learning rates and the piecewise learning rate on one subject in T1. The light grey shadow represents the searching region, and the light blue shadow represent the convergent region.

individuals and stabilizing the performance indicators at the desired level. In addition, the results of interactive force indicate that the customized robotic assistance can realize a stable interactive environment.

However, there are still some limitations to this study. First, the training tasks are defined only in a two-dimensional space, while most activities of daily living belong to the category of three-dimensional space. Second, the design of fuzzy rules mainly relies on subjective experiences, and as such, a more objective method should be involved to define the rules. Third, it is considered that the proposed performance evaluation method needs further investigation, and the parameter assignments warrant optimization in future studies.

In the future work, the training tasks will be extended to three-dimensional space, and more bilateral upper limb training modes will be considered. Besides, the fuzzy based method will be further improved with deep learning techniques to adjust membership functions and fuzzy rules, which can optimize robotic assistance. In addition, more performance indicators will be involved to make the evaluation of the limbs' motion function more accurate, such as joint angle, muscle activation and oxygen consumption. Based on above improvements, this work will be further verified on a number of patients suffered from motor disability of limbs.

V. CONCLUSION

In this paper, a performance-based iterative learning control strategy is proposed to optimize robotic assistance and improve subjects' engagement. Three clinical scale related performance indicators with a fuzzy logic are used to synthetically and quantitatively evaluate human users' motor functions, and a piecewise learning rate based iterative method is developed to adaptively converge to an appropriate assistance level. The experimental results demonstrate that the proposed control strategy can prompt acquisition of appropriate subject-specific

parameters within various training situations.

REFERENCES

- [1] R. J. Adams *et al.*, "Virtual activities of daily living for recovery of upper extremity motor function," *IEEE Trans. Neural Syst. Rehabil. Eng.*, vol. 26, no. 1, pp. 252-260, Jan. 2018.
- [2] D. J. Lin, S. P. Finklestein, and S. C. Cramer, "New directions in treatments targeting stroke recovery," *Stroke*, vol. 49, no. 12, pp. 3107-3114, Dec. 2018.
- [3] M. Park *et al.*, "Effects of virtual reality-based planar motion exercises on upper extremity function, range of motion, and health-related quality of life: a multicenter, single-blinded, randomized, controlled pilot study," *J. NeuroEng. Rehabil.*, vol. 16, no. 1, p. 13, Oct. 2019.
- [4] B. Zhong, W. Niu, E. Broadbent, A. McDaid, T. Lee, and M. Zhang, "Bringing psychological strategies to robot-assisted physiotherapy for enhanced treatment efficacy," *Front. Neurosci.*, vol. 13, p. 984, Sep. 2019.
- [5] H. I. Krebs, N. Hogan, M. L. Aisen, and B. T. Volpe, "Robot-aided neurorehabilitation," *IEEE Trans. Rehabil. Eng.*, vol. 6, no. 1, pp. 75-87, Mar. 1998.
- [6] X. Wu, D. Liu, M. Liu, C. Chen, and H. Guo, "Individualized gait pattern generation for sharing lower limb exoskeleton robot," *IEEE Trans. Autom. Sci. Eng.*, vol. 15, no. 4, pp. 1459-1470, Oct. 2018.
- [7] Q. Miao, A. McDaid, M. Zhang, P. Kebria, and H. Li, "A three-stage trajectory generation method for robot-assisted bilateral upper limb training with subject-specific adaptation," *Rob. Auton. Syst.*, vol. 105, pp. 38-46, Jul. 2018.
- [8] Q. Miao, Y. Peng, L. Liu, A. McDaid, and M. Zhang, "Subject-specific compliance control of an upper-limb bilateral robotic system," *Rob. Auton. Syst.*, vol. 126, p. 103478, Apr. 2020.
- [9] B. Zhong, J. Cao, A. McDaid, S. Q. Xie, and M. Zhang, "Synchronous position and compliance regulation on a bi-joint gait exoskeleton driven by pneumatic muscles," *IEEE Trans. Autom. Sci. Eng.*, vol. 17, no. 4, pp. 2162-2166, Oct. 2020.
- [10] L. Marchal-Crespo and D. J. Reinkensmeyer, "Review of control strategies for robotic movement training after neurologic injury," *J. NeuroEng. Rehabil.*, vol. 6, p. 15, Jun. 2009.
- [11] T. Proietti, V. Crocher, A. Roby-Brami, and N. Jarrassé, "Upper-limb robotic exoskeletons for neurorehabilitation: A review on control strategies," *IEEE Rev. Biomed. Eng.*, vol. 9, pp. 4-14, Apr. 2016.
- [12] Q. Miao, M. M. Zhang, J. H. Cao, and S. Q. Xie, "Reviewing high-level control techniques on robot-assisted upper-limb rehabilitation," *Adv. Rob.*, vol. 32, no. 24, pp. 1253-1268, Dec. 2018.
- [13] Z. Warraich and J. A. Kleim, "Neural plasticity: the biological substrate for neurorehabilitation," *Pm&R*, vol. 2, no. 12, pp. S208-S219, Dec. 2010.
- [14] P. R. Culmer *et al.*, "A control strategy for upper limb robotic rehabilitation with a dual robot system," *IEEE/ASME Trans. Mechatron.*, vol. 15, no. 4, pp. 575-585, Aug. 2010.
- [15] W. He, C. Xue, X. Yu, Z. Li, and C. Yang, "Admittance-based controller design for physical human-robot interaction in the constrained task space," *IEEE Trans. Autom. Sci. Eng.*, pp. 1-13, Oct. 2020.
- [16] G. Xu and A. Song, "Fuzzy variable impedance control for upper-limb rehabilitation robot," in *Adv. Intell. Sys. Comput.*, Oct. 2008, vol. 3, pp. 216-220.
- [17] M.-S. Ju, C.-C. Lin, D.-H. Lin, I.-S. Hwang, and S.-M. Chen, "A rehabilitation robot with force-position hybrid fuzzy controller: hybrid fuzzy control of rehabilitation robot," *IEEE Trans. Neural Syst. Rehabil. Eng.*, vol. 13, no. 3, pp. 349-358, Sep. 2005.
- [18] G. Z. Xu, A. G. Song, and H. J. Li, "Adaptive impedance control for upper-limb rehabilitation robot using evolutionary dynamic recurrent fuzzy neural network," *J. Intell. Robot. Syst.*, vol. 62, no. 3-4, pp. 501-525, Jun. 2011.
- [19] J. Bai, A. Song, T. Wang, and H. Li, "A novel backstepping adaptive impedance control for an upper limb rehabilitation robot," *Comput. Electr. Eng.*, vol. 80, p. 106465, Dec. 2019.
- [20] M. Zhang *et al.*, "Adaptive patient-cooperative control of a compliant ankle rehabilitation robot (CARR) with enhanced training safety," *IEEE Trans. Ind. Electron.*, vol. 65, no. 2, pp. 1398-1407, Feb. 2018.
- [21] W. M. dos Santos and A. A. G. Siqueira, "Optimal impedance via model predictive control for robot-aided rehabilitation," *Control Eng. Pract.*, vol. 93, p. 106465, Dec. 2019.
- [22] M. Zhang, A. McDaid, A. J. Veale, Y. Peng, and S. Q. Xie, "Adaptive trajectory tracking control of a parallel ankle rehabilitation robot with joint-space force distribution," *IEEE Access*, vol. 7, pp. 85812-85820, 2019.
- [23] A. U. Pehlivan, D. P. Losey, and M. K. O'Malley, "Minimal assist-as-needed controller for upper limb robotic rehabilitation," *IEEE Trans. Rob.*, vol. 32, no. 1, pp. 113-124, Feb. 2016.
- [24] L. Luo, L. Peng, C. Wang, and Z.-G. Hou, "A greedy assist-as-needed controller for upper limb rehabilitation," *IEEE Trans. Neural Networks Learn. Syst.*, vol. 30, no. 11, pp. 3433-3443, Nov. 2019.
- [25] P. Agarwal and A. D. Deshpande, "Subject-specific assist-as-needed controllers for a hand exoskeleton for rehabilitation," *IEEE Rob. Autom. Lett.*, vol. 3, no. 1, pp. 508-515, Jan. 2018.
- [26] Y. Zhang, S. Li, K. J. Nolan, and D. Zanotto, "Adaptive assist-as-needed control based on actor-critic reinforcement learning," in *Proc. Of the IEEE/RSJ Int. Conf. Intell. Robot. Syst. (IROS)*, Nov. 2019, pp. 4066-4071.
- [27] H. I. Krebs, J. J. Palazzolo, L. Dipietro, B. T. Volpe, and N. Hogan, "Rehabilitation robotics: performance-based progressive robot-assisted therapy," *Auton. Robot.*, vol. 15, no. 1, pp. 7-20, Jul. 2003.
- [28] E. Papaleo, L. Zollo, L. Spedaliere, and E. Guglielmelli, "Patient-tailored adaptive robotic system for upper-limb rehabilitation," in *Proc. IEEE Int. Conf. Robot. Automat. (ICRA)*, May. 2013, pp. 3860-3865.
- [29] C. Bosecker, L. Dipietro, B. Volpe, and H. I. Krebs, "Kinematic robot-based evaluation scales and clinical counterparts to measure upper limb motor performance in patients with chronic stroke," *Neurorehabil. Neural Repair*, vol. 24, no. 1, pp. 62-69, Jan. 2010.
- [30] C. Ott, R. Mukherjee, and Y. Nakamura, "A hybrid system framework for unified impedance and admittance control," *J. Intell. Robot. Syst.*, vol. 78, no. 3-4, pp. 359-375, Jun. 2015.
- [31] P. M. Fitts and J. R. Peterson, "Information capacity of discrete motor responses," *J. Exp. Psychol.*, vol. 67, no. 2, pp. 103-112, 1964.
- [32] T. Flash and N. Hogan, "The coordination of arm movements: an experimentally confirmed mathematical model," *J. Neurosci.*, vol. 5, no. 7, pp. 1688-1703, 1985.
- [33] W. Pedrycz, "Why triangular membership functions?" *Fuzzy Sets Syst.*, vol. 64, no. 1, pp. 21-30, May. 1994.
- [34] E. H. Mamdani and S. Assilian, "An experiment in linguistic synthesis with a fuzzy logic controller," *Int. J. Hum. Comput. Stud.*, vol. 51, no. 2, pp. 135-147, Aug. 1999.